AUTONOMOUS ORBIT CONTROL PROCEDURE, USING A SIMPLIFIED GPS NAVIGATOR AND A IMPROVED GROUND TRACK PHASE DRIFT PREDICTION METHOD, APPLIED TO THE CBERS SATELLITE

Roberto Luiz Galski[(1)], **Valcir Orlando**[(2)]
[(1) (2)] *CRC/INPE, Av. Astronautas 1758, São José Campos, SP, Brazil, +55 12-3208-6386, galski@ccs.inpe.br, +55 12-3208-6374, valcir@ccs.inpe.br*

Abstract: *In this paper, a periodic variation detected in the longitude phase drift first derivative of a sun-synchronous satellite (CBERS) is modeled and filtered, aiming at improving the performance of the autonomous satellite orbit control procedure presented by the authors in a previous work [1]. This new filtering process can be thought of as being a second smoothing layer applied to the ground track drift first derivative. This is done with the help of a curve fitting process, where an algebraic expression is used to match the time evolution curve resulting from the first smoothing layer. In this way, the curve fitting becomes an optimization process where one wishes to find out what are the values of the considered algebraic expression that best minimize the residuals between the two curves. Here, these parameters are found with help of an Evolutionary Algorithm. As a bonus, the mentioned procedure also provides another way to determine the value of the second time derivative of the longitude phase drift at Equator. Moreover, it was possible to discover that the fourth coefficient of the geopotential is the main source of the periodic variation present in the longitude phase drift first derivatives. The behavior of the whole system is evaluated by means of simulations of a CBERS-like phased remote sensing satellite orbits for both realistic and worst case conditions of solar activity.*

Keywords: *autonomous orbit control, autonomous navigation, ground track drift estimation, parameter optimization*

1 Introduction

In a former study [1], it was analyzed a version of an autonomous orbit control procedure that makes use of improved orbit estimates provided by a simplified GPS-based navigator [2] and of variable amplitude semi-major axis corrections, in order to keep the ground track phase drift at the Equator, D, of a CBERS-like sun-synchronous satellite within its allowed variation range. The CBERS (China-Brazil Earth Resources Satellite) satellite program is a Chinese-Brazilian project aimed at the monitoring of Earth's natural resources. The approach used in [1] calculates the semi-major axis maneuver amplitude in order to maximize the time between consecutive maneuvers and minimizing, in this way, the maneuver application number. For sun-synchronous orbit satellites in phase with the Earth's rotation, D is the parameter that presents the higher frequency of corrective maneuvers application. A polynomial approach [3] recently proposed to calculate the second time derivative of the ground track phase drift, $\ddot{D}$, of such kind of satellites was also used in that former article [1]. It helped reducing the uncertainty present in the computed $\ddot{D}$, allowing more precise calculations of the semi-major axis maneuver amplitudes and contributing to reduce the number of applied maneuvers, as originally desired.

The simplified GPS navigator improves the nominal geometric navigation solution provided by GPS receivers. This is done by directly using the GPS solution as input (observations) for a real time Kalman filtering process. The orbital state vector has been extended in order to include the systematic error that is imposed to the GPS geometric solution by the changes in the set of satellites which are visible to the receiver.

The investigation of the results obtained in the previous work [1] allowed to observe that, even after the application of a smoothing procedure, a periodic variation has still remained in the computed first time derivative of the ground track phase drift, $\dot{D}$. Since this derivative is needed to foresee the time evolution of the ground track phase drift itself, it shall be accurately estimated. The precise

knowledge of the future time evolution of the ground track drift is required if one intends to increment the degree of confidence of the orbit maneuver computation process.

One observed that the period of the mentioned cyclic variation on $\dot{D}$ was of about one day. It was also verified that this periodic variation has the geopotential as its main source.

In this article, the cyclic perturbation on the smoothed $\dot{D}$ is presented, studied and a filtering procedure for it is proposed. The filtering procedure makes use of a curve fitting process, where a line plus sine formula is used to generate an approximate curve for the cyclic perturbation curve of $\dot{D}$. Next, the parameters of the formula that defines the approximate curve are varied until it matches the original curve. In this way, the curve fitting process becomes an optimization process where the parameters of the approximate curve are the unknown variables and one desires to find out what are the parameters values that best minimize the residuals between the two curves. Here, these parameters are found with the help of a hybrid Evolutionary Algorithm. The GEO + ES algorithm [5] was applied to the problem, in order to conjugate the good convergence properties of the Generalized Extremal Optimization - GEO [6] algorithm with the self-tuning characteristics present in the Evolution Strategies – ES methods [7]. As a bonus, the mentioned procedure also provides another way to determine good estimates of $\ddot{D}$.

The behavior of the system is evaluated by means of numeric simulation of CBERS-like phased remote sensing satellite orbits. For the CBERS satellite series the maximum allowable variation range for D is ±4km. The aim of the paper is to verify the impact the addition of a second smoothing layer applied to $\dot{D}$ has on the performance of the entire autonomous control system, when compared to the results already obtained for the same satellite in the previous works. Both realistic and worst case conditions in terms of solar activity were considered in the simulation.

2. The Cyclic Perturbation, Its Source and the Proposed Filter

In an attempt to find out what was causing the cyclic perturbation on $\dot{D}$ a realistic orbit propagation software were run several times. On each one of these runs a specific perturbation source routine was deactivated, such as sun and moon gravitational attraction, solar radiation pressure, atmospheric drag, and, finally, the number of terms used in the geopotential force model. It turned out that this last one was, in fact, the source of the cyclic perturbation seen on $\dot{D}$, as it can be seen with help of Figure 1.a. It shows the behavior of the time evolution of when the geopotential coefficients are successively added to the orbit simulation process. As it can be observed, when terms up to J_4 are added the cyclic perturbation appears, fact that remains true for higher order terms. Apart from selectively deactivating the perturbation sources as just described, the methodology used to calculate the smoothed observations of $\dot{D}$ presented in Fig. 1.a is the same one already described in [1].

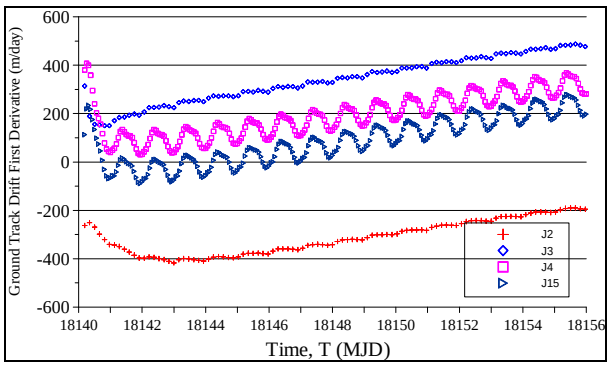

Figure 1.a - Effect of the Geopotential on $\dot{D}$

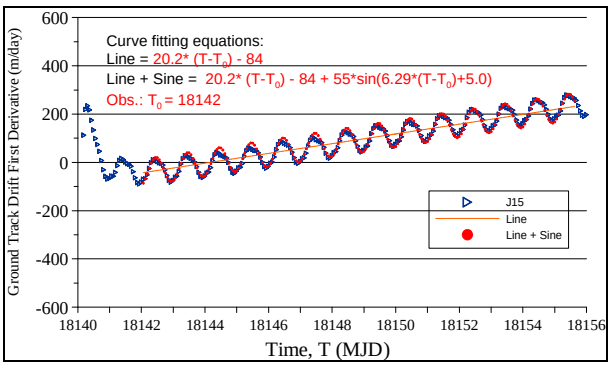

Figure 1.b - Filtering Equations for $\dot{D}$

Further investigation has shown that the frequency of this cyclic perturbation remains the same during the entire simulation interval (one year) and for both moderate and critical solar conditions used in this paper (see section 4). Only the amplitude of the oscillation varies, the higher ones occurring with critical solar condition. This fact motivated the development of the filtering

procedure presented here. As can be seen in Fig. 1.b, most of the cyclic perturbation is easily modeled by the sum of an inclined line and a sine. Then, the filter model takes the following equation:

$$\dot{D}_f(\mathbf{x}, t) = x_1 \cdot t + x_2 + x_3 \cdot \mathrm{Sin}(x_4 \cdot t + x_5) \tag{5}$$

where $\dot{D}_f$ is the value of $\dot{D}$ predicted by the filter at a given time instant, t (days); x_1 is the line slope, in m/day^2; x_2 is the line value at $t=T_0$, in m/day (T_0=18142 in the example given in Fig. 1.b); x_3 is amplitude of the cyclic perturbation, in m/day; x_4 is the frequency of the cyclic perturbation, in rad/day and x_5 is the angular phase of the cyclic perturbation, in rad. In Eq. 5, the x values are the unknowns of the curve fitting process. The optimal x values, that is, the values of the x variables that produce the best match among the filter model curve and observed data of $\dot{D}$, will be computed in the sense of minimizing the sum of squared residuals. Mathematically:

$$\text{Minimize} \quad F(\mathbf{x}) = \sum_{t=t_{k-n}}^{t=t_k} r(t)^2 = \sum_{t=t_{k-n}}^{t=t_k} (\dot{D}_f(\mathbf{x}, t) - \dot{D}(t))^2 \tag{6}$$

$$\text{Subject to:} \quad \mathbf{x_{min}} <= \mathbf{x} <= \mathbf{x_{max}}$$

Eq. 6 represents an optimization problem where the objective function to be minimized, F(**x**), is the sum of the squared residuals, r(t). Considering that t_k is the time instant of the most recent observation of $\dot{D}$, the time interval for the curve fitting is chosen by means of n, the number of observation samples of $\dot{D}$ previous to t_k that will be considered.

3. Autonomous Control Procedure Overview

A block diagram of the autonomous control system considered in the present article is given in Figure 2. It gives an overview of the full simulation loop.

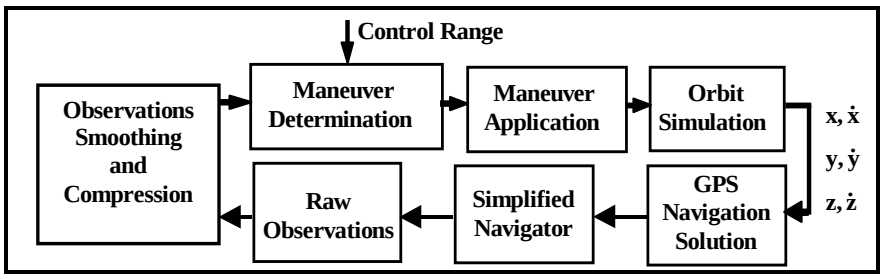

Figure 2. Block Diagram of the Autonomous Control System

Except by the new filtering procedure for $\dot{D}$, the control system is basically the same already described and used in [1]. For this reason, here, only a brief description will be given. The precise orbit estimates provided by the realist orbit propagation (Orbit Simulation block) are used in the block "GPS Navigation Solution", where random and bias errors equivalent to those of the real GPS estimates are added to the precise orbit estimates. In [1], root mean square random errors of 100m in position and 1m/s in velocity and systematic variations (bias) with values of the order of 100m and duration of about 1 to 15 minutes were used for the coarse GPS geometric estimates. The same values are used in the present article. The Simplified Navigator takes the position components of the GPS Navigation Solution as inputs and refines them by means of a Kalman filtering process which incorporates a procedure for automatic treatment of observation biases. Next, Raw Observations of the ground track drift are computed from each set of improved orbit estimates supplied by the simplified navigator. These raw observations are preprocessed in real time by the block "Observations Smoothing and Compression", in order to achieve data smoothing and redundancy reduction. The new filtering procedure by curve fitting for $\dot{D}$ presented in this article is applied in this block and allows also obtaining filtered values of $\ddot{D}$. Finally, the computed observations of D, $\dot{D}$, and $\ddot{D}$ are used within the Maneuver Determination process, where the instants of orbit correction applications are defined and their respective amplitudes calculated. Here, unlike what was done in [1], information about K_p and $F_{10.7}$ are no longer furnished to this block, but only the

control ranges. Once defined the need of a maneuver, its execution occurs within the block "Maneuver Application", where its amplitude and the corresponding changes in the orbital parameters of the satellite are calculated and imposed, closing the simulation loop.
The following two conditions are used to verify the need of a corrective maneuver:

$$\overline{D}(t_M) > D_{max} - ns.\sigma(t_M) \text{ or} \quad (1)$$

$$\overline{D}(t_{M+1}) > D_{max} - ns.\sigma(t_M) \quad (2)$$

where $\overline{D}(t_M)$ and $\overline{D}(t_{M+1})$ are the smoothed values for D at instants t_M and t_{M+1}, respectively. D_{max} is a previously chosen control limit; $\sigma(t_M)$ is the standard deviation of $\overline{D}(t_M)$; t_M is the time instant of the last (m-th) observation sample of $\overline{D}$ known and ns is a real number. The idea behind condition 2 is to use it to apply a maneuver at an instant t_M if the estimated value for the ground track drift at t_M is less than the allowed limit but the value foreseen for t_{M+1}, the next maneuver verification moment, is greater than the allowed limit. The smoothed value $\overline{D}(t_M)$ is obtained from the raw values of D by means of the same weighted moving average procedure [4] described and used in [1]. By its turn, the raw observations of D are computed from the orbit estimates issued by the simplified navigator using:

$$D = a_e \cdot [\Delta\Omega + \frac{\Delta\alpha}{(N + P/Q)}] \quad (3)$$

where a_e is the mean Equator radius, $\Delta\Omega$ is the right ascension of the ascending node deviation from the reference value; $\Delta\alpha$ is argument of latitude deviation from the reference value; N, P and Q are three integer numbers used to define the number of orbit revolutions completed by the satellite in one day, including its fractional part. The argument of latitude itself is given by $\alpha = \omega + M$, the sum of the perigee argument and the mean anomaly of the satellite, respectively.
The future estimate for $\overline{D}(t_{M+1})$ is calculated assuming constant solar flux during the time interval between two successive maneuvers, which implies in having constant $\dot{a}$ (a being the orbit semi-major axis) and parabolic time evolution curve for D. Mathematically:

$$\overline{D}(t_{M+1}) = \overline{D}(t_M) + \dddot{\overline{D}}(t_M)\,\Delta t + 1/2\ \ddot{\overline{D}}(t_M)\,(\Delta t)^2 \quad (4)$$

where $\Delta t = t_{M+1} - t_M = \Delta t_{CS}$ is the elapsed time among two successive compressed samples of $\overline{D}$ supplied to the "Maneuver Determination" block by the "Observations Smoothing and Compression" block (see Figure 2), Δt_{CS}, being the time window considered for the observations of $\overline{D}$, considered in the compression process. It is important to mention that the block "Observations Smoothing and Compression" receives samples of D from "Raw Observations" block and calculates the smoothed $\overline{D}$ values at a pace given by the time interval Δt_S and supplies samples of $\overline{D}$ to the "Maneuver Determination" block at a pace given by the time interval Δt_{CS}, where $\Delta t_{CS} > \Delta t_S$ (usually $\Delta t_{CS}/\Delta t_S > 10$). The value of $\dddot{\overline{D}}(t_M)$ is obtained from a three-stage procedure, of the block "Observations Smoothing and Compression". These three stages are the followings: i) $\dot{D}$ values are numerically calculated; ii) $\dot{D}$ values are smoothed, generating $\dot{\overline{D}}$; iii) $\dot{\overline{D}}$ values are filtered, generating $\ddot{\overline{D}}$. The values of $\dot{D}$ are calculated using:

$$\dot{D}(t_k) = \left(\overline{D}(t_k) - \overline{D}(t_{k-1})\right) / \left(t_k - t_{k-1}\right) \quad (5)$$

where $t_k - t_{k-1} = \Delta t_S$ is the elapsed time among two successive samples of $\overline{D}$. By its turn, the values of $\overline{D}$ at the instants t_{k-1} and t_k are obtained by smoothing the values of D supplied to the "Observations Smoothing and Compression" block by the "Raw Observations" block at the same instants. Next, $\dot{D}(t_k)$ values are smoothed using the same weighted moving average procedure [4] used for D, generating the values of $\dddot{\overline{D}}(t_k)$. Finally, the filtering procedure described in section 2 is applied. After choosing a time interval for the filter, Δt_F, the corresponding number of data samples, n, is calculated from $n = INT(\Delta t_F/\Delta t_S)$ and the GEO+ES [5] algorithm is applied to the minimization

problem defined in Eq. 6, retrieving **x***, the best solution found for the filter. Among the components of **x***, x_1^* corresponds to $\overline{\overline{\dot{D}}}(t_k)$, the filtered value of $\ddot{D}(t_k)$. In this way, $\overline{\overline{\ddot{D}}}(t_k)$ is directly obtained from filtering the values of $\overline{\dot{D}}(t_k)$. From **x***, one also has $x_2^* = \overline{\overline{\dot{D}}}(t_{k-n})$, the filtered value for the first derivative of the ground track drift at the instant, t_{k-n}, that is, at the beginning of the filtering interval ($t_{k-n}=T_0=18142$, in the example of Fig. 1.b). The value of $\overline{\overline{\dot{D}}}(t_k)$ is taken as the value of the linear component of the fitted curve in the time t_k:

$$\overline{\overline{\dot{D}}}(t_k) = \overline{\overline{\dot{D}}}(t_{k-n}) + \overline{\overline{\ddot{D}}}(t_k) \cdot \Delta t_F = x_2^* + x_1^* \cdot \Delta t_F \tag{6}$$

It is worth mentioning that $\overline{\overline{\dot{D}}}(t_k)$ and $\overline{\overline{\ddot{D}}}(t_k)$ values are calculated after constant time intervals equal to Δt_S (that is: $\Delta t_S = t_{k+1} - t_k$ = constant) and when the number of Δt_S intervals matches Δt_{CS}, the corresponding values of $\overline{\overline{\dot{D}}}(t_k)$ and $\overline{\overline{\ddot{D}}}(t_k)$ are taken as the values of $\overline{\overline{\dot{D}}}(t_M)$ and $\overline{\overline{\ddot{D}}}(t_M)$, that is: the input values of the "Maneuver Determination" block, used in Eq. 4. For the time interval when the filter is not yet being applied to the $\overline{\dot{D}}$ data (just after a maneuver execution, for instance), the values of $\overline{\dot{D}}(t_k)$ are supplied to the "Maneuver Determination" block, instead of the value of $\overline{\overline{\dot{D}}}(t_k)$, which is not yet available. In these cases, for replacing the missing $\overline{\overline{\ddot{D}}}(t_k)$, the polynomial method proposed in [3] is used in order to calculate $\ddot{D}(t_k)$ estimates. For this aim, it is considered that the onboard autonomous control system of the satellite allows the reception of the required values of K_p and $F_{10.7}$ as inputs, which are provided by internal sensors or by telecommand from the ground.

Only the application of positive corrections to the orbit semi-major axis is considered for the maintenance of D inside the control ranges. Each semi-major axis increment to be applied to the satellite orbit is computed with the aim of changing the value of $\dot{D}$ such that the further minimal value of D, after the maneuver application, be equal to a previously chosen inferior limit, D_{min}. The maximization of the time interval between the executions of two successive maneuvers is implicit in this strategy.

Considering some approximations which can be assumed for phased sun-synchronous orbits like, the maneuver size in terms of semi-major axis variation, Δa, is calculated by [8]:

$$\Delta a = -\frac{T_{te}}{3\pi}\frac{a_R}{a_e}\left(\overline{\dot{D}}(t_M^+) - \overline{\dot{D}}_C(t_M^-)\right) \tag{7}$$

where T_{te} is the average solar day (86400s=1day); a_R is the semi-major axis of the reference orbit, a_e is the mean Equator radius and $\overline{\dot{D}}_C(t_M^-)$ is the last preprocessed value of $\overline{\overline{\dot{D}}}$. Case $\overline{\overline{\dot{D}}}$ is not available, $\overline{\dot{D}}$ is used instead. $\overline{\dot{D}}(t_M^+)$ is calculated with help of the following equation (adapted from [9]):

$$\overline{\dot{D}}(t_M^+) = -\sqrt{2\ \overline{\overline{\ddot{D}}}(t_M^+)\ \left(\overline{D}(t_M^+) - D_{min}\right)} = -\sqrt{2\ \overline{\overline{\ddot{D}}}(t_M)\ \left(\overline{D}(t_M) - D_{min}\right)} \tag{8}$$

where D_{min} is a previously specified inferior limit of the allowed variation range of D.

Then, the tangential velocity increment, ΔV_T, is finally calculated by:

$$\Delta V_T = \frac{\Delta a}{2\,a_R} V \tag{9}$$

where V is the magnitude of the velocity vector of the satellite.

4. Autonomous Control Test Results

The performance of the autonomous orbit control procedure just proposed was verified through the execution of a realistic simulation of its application to a CBERS-like satellite, in the same way it was done in [1]. Figure 3 shows the solar profiles considered in the simulation.

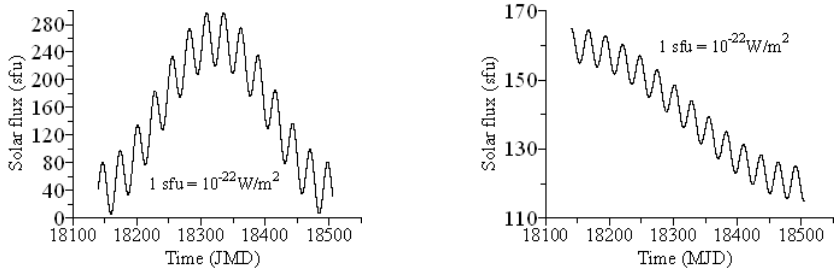

Figure 3. Critical and Moderate Solar Profiles Considered in the Tests

A maximal rate of about one maneuver application per orbit period (~100 min) was imposed. It was also considered a GPS observation rate (and consequently the navigator output rate) of one estimate each nine seconds. Only one among sixty orbit estimates sets successively issued by the navigator is used by the control system (meaning a rate of one data each nine minutes, that is, Δt_S = 9min). . After each autonomous maneuver execution the smoothing processes [4] applied to D and $\dot{D}$ were restarted, in the same way it was done in [1]. In these processes the time windows of 8h and 40h were used for D and $\dot{D}$, respectively. The same time windows were used for moderate and critical solar activity conditions. All other parameters of the smoothing not explicitly mentioned here were set as in [1]. Time intervals of 12 and 5 days with no maneuver occurrences were observed, respectively for moderate and critical solar activity scenarios. The vectors $\mathbf{x_{min}}$ = [-200, -1500, 10, 6.2, 0.0] and $\mathbf{x_{max}}$ = [200, 1500, 100, 6.4, 2π] were used in Eq. 6. Within the autonomous control simulation loop, the GEO + ES algorithm was run each time it was necessary to find the parameters of the filter used for estimating the smoothed values for $\dot{D}$ (section 2). Since a maneuver, in general, imposes a significant change in $\dot{D}$, the only restriction observed in the filter application is to collect enough amount of data, i.e., a time interval without maneuvers greater than Δt_F. For each run, a thousand generations were allowed to occur within the algorithm and this limit was used as a stopping criterion. Three mutations per variable were used, so l_j=l=3. The limits for varying b were set to b_{MIN}=1.05 and b_{MAX}=10. The values of δ=0.0 and of α=0.3 were used. The four parameters just mentioned are internal parameters for GEO + ES.

The results of the current study, considering moderate solar activity condition, are shown in Fig.s 4 and 6 for the ground track drift time evolution and the semi-major axis maneuvers, respectively. For comparison purposes, Fig.s 5 and 7 present the results obtained in [1] for the same conditions.

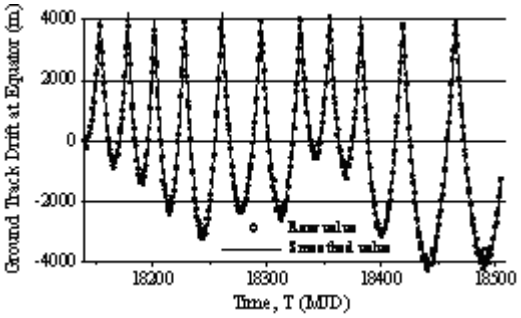

Figure 4. Ground Track Drift

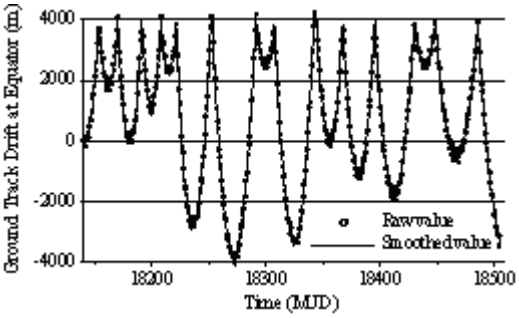

Figure 5. Ground Track Drift from [1]

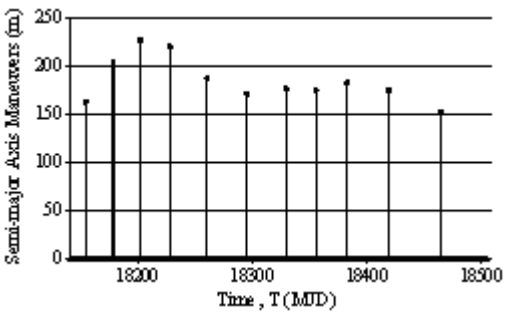

Figure 6. Maneuvers

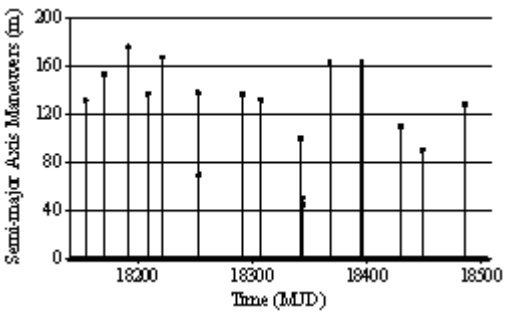

Figure 7. Maneuvers from [1]

The values D_{max}=3,800m and ns=0 were used in Conditions 1 and 2, considering D_{min}=-3,800m in Eq. 8. Time intervals of 8h and 40h were used for smoothing D and $\dot{D}$, respectively. For the filter, Δt_F = 5 days was taken. Eleven maneuvers has occurred, with an accumulated Δa for the period of 2,034.7m. The major maneuver had Δa=226.8m and the minor Δa=152.9m. From Fig. 4, it is possible to see that, for the moderate solar activity profile, the new autonomous control version used the very limit of the ±4km allowed variation range for D in order to reduce the amount of applied maneuvers. When compared with previous results, one can see that there was a substantial reduction in the number of applied maneuvers, since in [1], 17 maneuvers were needed against only 11 maneuvers in the current case. In terms of the accumulated Δa, both results are practically the same (2,092.4m in [1] against 2,034.7m here).

The results of the current study, when moderate solar activity condition was considered, are shown in Fig.s 8 and 10, for the ground track drift time evolution and the semi-major axis maneuvers, respectively. For comparison purposes, Fig. 9 and Fig. 11 present the results obtained in [1] for the same conditions. The values D_{max}=3,800m and ns=0 were used in Conditions 1 and 2, and D_{min}=-3,800m in Eq. 8. The values 8h and 40h were used for smoothing D and $\dot{D}$, respectively. For the filter, Δt_F = 15 days was used. The number of maneuvers was 14 with an accumulated Δa for the period of 2,959.3m. The major maneuver had Δa=342.1m and the minor Δa=90.4m. From Fig. 4, it is possible to see that, for the critical solar activity profile, the new autonomous control version also respected the very limit of the ±4km (allowed variation range for D) in order to reduce the amount of applied maneuvers. When compared with previous results, one can see that the reduction in the number of applied maneuvers is even more substantial than the one occurred for the moderate solar activity condition. Now, 14 maneuvers were needed against 26 maneuvers here. In terms of the accumulated Δa, both results are practically the same (2,953.0m in [1] against 2,959.3m here).

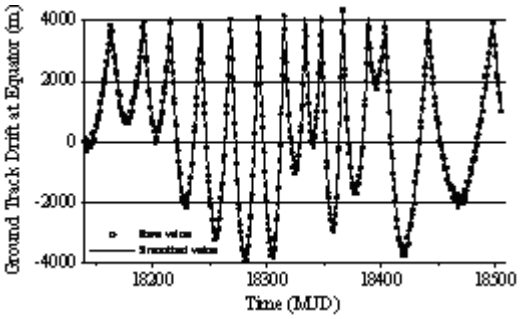

Figure 8. Ground Track Drift

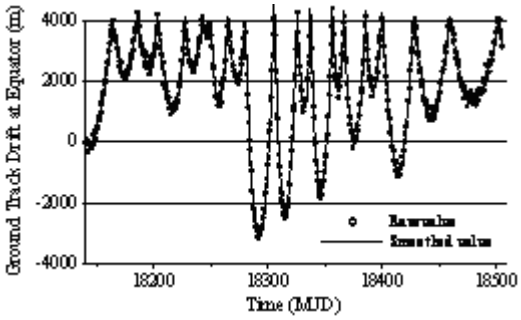

Figure 9. Ground Track Drift from [1]

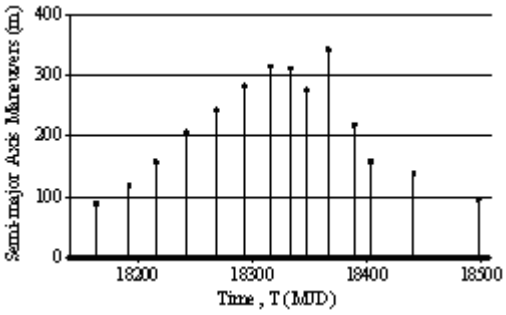

Figure 10. Maneuvers

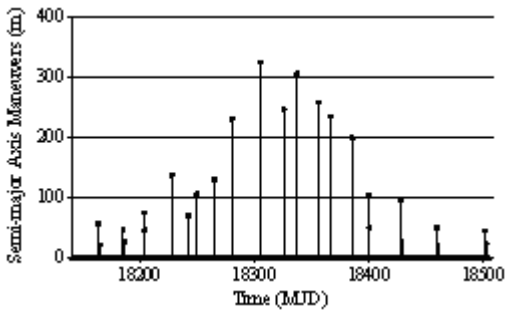

Figure 11. Maneuvers from [1]

5. Conclusions

In this article, it was analyzed a version of an autonomous orbit control procedure that makes use of improved orbit estimates provided by a simplified navigator. This procedure uses variable amplitude semi-major axis corrections in order to keep the ground track drift at equator of a CBERS-like satellite within the mission specified allowed variation range. A filter for a cyclic perturbation, which is present in smoothed estimates of the first derivative of the ground track drift, was

proposed, implemented and tested. The filter uses a curve fitting process whose parameters are computed with help of an Evolutionary Algorithm. The main conclusion is that the objectives were successfully achieved. The results of simulation tests accomplished with the new method shown it really has a good capability in removing the cyclic perturbation that is still present in the first derivative estimates of the ground track drift delivered by the previous application of algorithm presented in reference [1]. This feature improved the autonomous orbit control procedure performance the performance, since more accurate calculations of the semi-major axis maneuver amplitudes could be computed and the number of applied maneuvers could be reduced. The obtained results can be considered very satisfactory and promising.

6. References

[1] GALSKI, R. L.; ORLANDO, V. Autonomous Orbit Control Procedure, Using a Simplified GPS Navigator and a New Longitude Phase Drift Prediction Method, Applied to the CBERS Satellite. In: 22nd International Symposium on Spaceflight Dynamics, 2011, São José dos Campos, SP, Brazil. CD-ROM of 22nd ISSFD, 2011.

[2] GALSKI, R. L.; ORLANDO, V.; KUGA, H. K. Autonomous Orbit Control Procedure, Using a Simplified GPS Navigator, Applied to the CBERS Satellite. In: 16th International Symposium on Spaceflight Dynamics, 2001, Pasadena. CD-ROM of 16th ISSFD, 2001.

[3] ORLANDO, V.; KUGA, H. K.; GALSKI, R. L. . An Approach for Predicting the Effects of Solar Activity on the Evolution of Ground Track Drift of Phased Satellites. In: 21st International Symposium on Space Flight Dynamic - 21st ISSFD, 2009, Toulouse - France. 21st International Symposium on Space Flight Dynamic. Toulouse - France : CNES, 2009. p. 1-12.

[4] GALSKI, R. L., “Autonomous Orbit Navigator Development, Using GPS, Applied to Autonomous Orbit Control”, 162 p. (INPE-8982-TDI/813). (In Portuguese). Master Degree Dissertation on Space Mechanics and Control - Instituto Nacional de Pesquisas Espaciais, São José dos Campos, SP, Brazil. 2001. Available at: <http://urlib.net/sid.inpe.br/jeferson/2004/09.01.11.28>.

[5] GALSKI, R.L., “Development of Improved, Hybrid, Parallel and Multiobjective Versions of the Generalized Extremal Optimization Method and its Application to the Design of Spatial Systems”, 279 p. (INPE-14795-TDI/1238). D.Sc. Thesis (In Portuguese), Instituto Nacional de Pequisas Espaciais, Brazil, 2006. Available in:<http://urlib.net/sid.inpe.br/mtc-m17@80/2006/11.30.19.04>. Accessed in: 01 out. 2010.

[6] DE SOUSA, F.L., RAMOS, F.M., PAGLIONE, P., and GIRARDI, R.M. “New stochastic algorithm for design optimization”, AIAA Journal 41 (Number 9), pp. 1808-1818, 2003.

[7] EIBEN, A.E.; SMITH, J.E., “Introduction to evolutionary computing”, Springer-Verlag, Berlin, Germany, 2003.

[8] CARROU, J. P., “Space Flight Dynamics”, Cépaduès-Editions, ISBN: 2.85428.378.3, 1995.